Dalton Transactions

Accepted Manuscript

ROYAL SOCIETY OF CHEMISTRY

www.rsc.org/dalton

Dalton Transactions

RSCPublishing

PAPER

Bidentate NHC^Pyrozolate ligands in Luminescent Platinum(II) Complexes

Cite this: DOI: 10.1039/xoxxoooooox

Abbas Raja Naziruddin,[⊥] Anzhela Galstyan,[⊥] Adriana Iordache,[⊥] Constantin G. Daniliuc,[|] Cristian A. Strassert,*[,⊥] Luisa De Cola*[,⊥,▽]

Received 25th May 2014,
Accepted ooth XXXX 2014

DOI: 10.1039/xoxxoooooox

www.rsc.org/

A bidentate C^N donor set derived from a N-heterocyclic carbene (NHC) precursor linked to a trifluoromethyl (CF_3) functionalized pyrazole ring is described for the first time. The ligands have been employed to prepare four new phosphorescent complexes by coordination of platinum(II) centres bearing cyclometalated phenyl-pyridine/triazole-pyridine chelates. The electronic and steric environments of these complexes were tuned through incorporation of suitable substituents in the phenyl-pyridine/triazole-pyridine ligands, wherein the position of the phenyl–ring substituent (a CF_3 group) also directs the selective adoption of either *trans* or *cis* configuration between the C_{NHC} and the C_{phenyl} donor atoms. Molecular structures obtained by X-ray diffraction for three of the complexes confirm a distorted square-planar configuration around the platinum centre, and DFT calculations show that the substituents have a significant influence on the energies of the frontier orbitals. Moreover, a platinum(II) complex featuring the new bidentate NHC^pyrazolate ligand and a bulky adamantyl functionalized pyridine-triazole luminophore was observed to be highly emissive and exhibiting a sky-blue luminescence (λ_{Em} = 470 nm) with photoluminescence quantum yields as high as 50% in doped PMMA matrices. A complete photophysical investigation of all of the complexes in solution as well as in the solid state is herein reported.

INTRODUCTION

The ever increasing demand to save energy and the global awareness of the need to efficiently use fossil fuels has sparked the deployment of cleaner energy alternatives[1] and provoked the utilization of freely available natural feedstocks such as CO_2.[2] Extensive interest has also been laid to attain sustainability in lighting technology[3] by using emissive complexes as the primary building blocks for electroluminescent devices.[3c] Furthermore, motivation for this emerging technology also roots on the industrial demand for the fabrication of efficient flat panel displays.[4] The use of transition metal complexes as triplet emitters is advantageous, as they can deliver four-fold enhanced efficiencies, as compared to organic fluorophores.[5] Electroluminescent complexes based on iridium,[6] ruthenium,[7] rhenium,[8] osmium,[9] platinum,[10] gold,[11] copper,[12] and zinc,[13] have been previously well documented. Ligand design plays a pivotal role in determining the stabilities and luminescence efficiencies of these complexes. For example, symmetric NCN type benzene *bis*(pyrazolates)[10d] or unsymmetric NNN[14] type pincer ligands constituting rigid ligand frameworks exhibit rich photoluminescence upon coordination to platinum(II) or iridium(III) centers. Transition metal complexes bearing *N*-heterocyclic carbene (NHC) ligands are vastly applied in organometallic catalysis,[15] as their strong σ donor properties and large ligand cone angles facilitate the stabilization of the transition states, preventing the degradation of the involved catalytic species. These aspects also render them comparable to their phosphine counterparts.[16] More recently, several research groups[6a, 6c, 10h, i, 17] have dedicated extensive efforts to obtain photoactive complexes bearing NHC ligands as functional units. The strong ligand field of NHC ligands assists in destabilizing the otherwise thermally accessible yet non-emissive metal-centred d-d states in their complexes. Moreover, coordination of bidentate, tridentate or tetradentate-NHCs or mixed NHCs to the platinum atom renders a rigid coordination sphere that minimizes the vibronic deactivation of excited states and consequently affords high photoluminescence quantum yields (PLQY).[4]

Deep blue emission was observed in homoleptic platinum(II) complexes featuring *bis*(NHC) ligands.[18] Also complexes bearing cyclometallated pincer *bis*(carbene) ligands with phenylene linkers (^{R}CCC^{R})[19] or pyridyl linkers (^{R}CNC^{R})[20] exhibit blue emission along with vapochromic or aquachromic responses. Few rare examples of green–blue emitting heteroleptic Pt–NHC complexes that feature cyclometalation *via* the *N*-wingtip are known.[21] Iridium(III) or platinum(II)

based phosphors derived from *P^N*[22] or *P^O*[23] donor sets also emit blue light.[22] In the search for neutral platinum-based phosphors with green–blue emission, ligands bearing ring-fluorinated aromatic moieties should be avoided since they can easily degrade, and problems also arise when readily oxidizable phosphine donors are employed. Thus we have developed a mono-anionic bidentate NHC^pyrazolate ligand system to coordinate the platinum (II) center *via* a C^N donor set. By combining suitably functionalized phenyl-pyridine/pyridine-triazole luminophores with a NHC^pyrazolate ligand, four new heteroleptic platinum phosphors were synthesized. Structural, photophysical and electrochemical characteristics of these complexes are evaluated along with TD-DFT calculations.

Results and discussion

Synthesis and structural characterization

The ligand precursor (NHC^pyrazolate)H_2·Br (**7**), was obtained by reacting stoichiometric amounts of 1-methylbenzimidazole and the bromomethyl pyrazole derivative (**6**). Compound **6** was previously synthesized by a modified five step procedure (ESI†).[24] Schematically, the reaction of an adequate diketone derivative (**1**) and hydrazine hydrate in ethanol yielded an unsymmetrically substituted pyrazole (**2**). Oxidation of the methyl function of the pyrazole derivative into the respective carboxylic acid (**3**) was achieved *via* a standard procedure using $KMnO_4$ as the oxidant. Esterification of the carboxylic acid using H_2SO_4/methanol resulted in compound **4**. The ester derivative was further transformed into the corresponding alcohol (**5**) by reduction with $LiAlH_4$ in tetrahydrofuran (thf); which was subsequently brominated using an excess of PBr_3 with the formation of (**6**) (**Scheme 1**).[22]

The phenyl-pyridine ligand precursors were obtained *via* Suzuki coupling of the corresponding aryl-boronic acids and 2-bromopyridine in the presence of catalytic amounts of $[Pd(PPh_3)_4]$.[25] The pyridine-triazole ligand precursor (**8**) was obtained *via* modification of our previous protocol in which a bulky adamantyl group replaces the fluorinated aryl substituent.[26] Adequate cyclometallated phenyl-pyridine–Pt(II) precursors were synthesized according to literature procedures.[27] Alternatively, the (pyridine-triazole)–Pt(II) precursor [**12**] was obtained by heating equal stoichiometric amounts of compounds **8** and $[K_2PtCl_4]$ in a 2-ethoxyethanol–water mixture for 12 h at 85 °C.[26] Heteroleptic Pt(II) complexes [**9**], [**10**], [**11**] and [**13**] were obtained by reacting the ligand precursor **7** and the corresponding (μ-Cl) cyclometallated Pt(II) precursor or the (pyridine-triazole)–Pt(II) precursor [**12**] under reflux in methanol using triethylamine as base (**Scheme 2**).

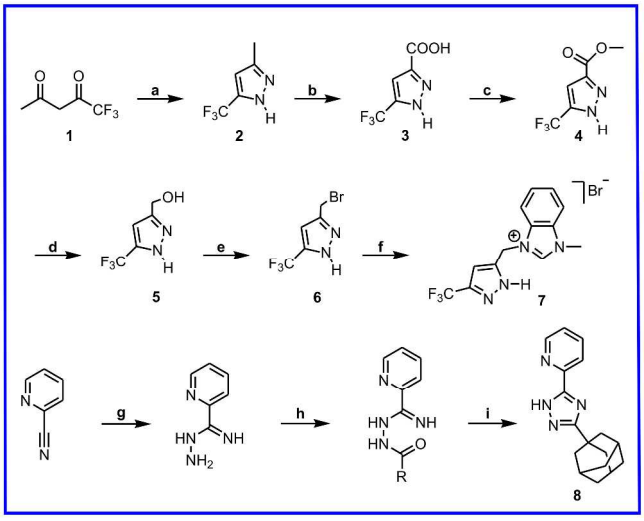

Scheme 1. Synthesis of the pyrazole-functionalized NHC ligand precursor **7**: a) hydrazine hydrate, reflux; b) $KMnO_4$/heat (oxidation); c) H^+/methanol (esterification); d) $LiAlH_4$/ thf (reduction); e) PBr_3/thf; f) 1-methyl benzimidazole. Synthesis of the adamantyl-functionalized pyridine-triazole ligand precursor **8**: g) hydrazine hydrate/ethanol; h) adamantylcarbonyl chloride, (R = adamantyl); i) 180 °C, ethylene glycol, 2 h.

All the complexes have been characterized using ^{1}H NMR, ^{13}C NMR, ^{19}F NMR, and high resolution mass spectrometry. In addition X-ray structural determination of the complexes [**9**], [**10**], and [**11**], was performed on single crystals (see below). The ^{1}H NMR spectra of complexes [**9**], [**10**], [**11**] and [**13**] were lacking the characteristic benzimidazolium-C2–*H* resonances, along with the absence of pyrazole N–*H* resonances that were observed in the free ligand **7**. In addition, chemically and magnetically equivalent CH_2 protons of the methylene bridges, that link the pyrazole ring and the NHC precursor of the uncoordinated-bidentate ligand **7**, were rendered diastereotopic upon complexation, due to the formation of a rigid metallocycle. The ^{1}H NMR signals of these diastereotopic protons were observed as two singlets at δ 5.43 and 5.30 ppm in [**9**], δ 5.41 and 5.39 ppm in [**10**] and δ 5.48 and 5.41 ppm in [**11**]. However only a doublet was observed at δ 5.35 ppm (J = 2.2 Hz) for [**13**]. The pyridine–α_H protons of the phenyl pyridine or triazole pyridine co-ligands also tend to be more acidic in all complexes, as confirmed by the down-field resonances observed at δ 10.01 and 10.22 ppm in complexes [**9**] and [**10**] respectively, and at δ 9.73 ppm in [**11**] and [**13**]. Formation of the complexes was also confirmed by the ^{13}C NMR spectra, in which the carbenoid carbon resonances appeared at δ 168.7, 166.5, 166.0 and 174.3 ppm for the complexes [**9**], [**10**], [**11**] and [**13**] respectively. ^{13}C NMR resonances of the methylene bridge (–*C*H_2–), that links the pyrazole ring and the NHC donor of the coordinated NHC^pyrazolate ligand, were observed in the range of δ 42.6–44.3 ppm in all of the complexes. In addition, ^{19}F NMR resonances of pyrazole–CF_3 substituent were observed at δ –60.52 and –60.89 ppm in complexes [**9**] and [**13**] respectively. Complexes, [**10**] and [**11**] bearing two additional CF_3 substituents on the phenyl ring, revealed in the ^{19}F NMR spectra three resonances at δ –57.36, –60.49, –63.16 ppm and δ –58.63, –60.61, –62.85 ppm, respectively.

Single crystals of complexes [**9**], [**10**] and [**11**] were obtained by slow diffusion of hexane vapors into their dichloromethane solutions at ambient temperature. The molecular structures of [**9**], [**10**] and [**11**] are depicted in **Figure 1** and selected bonding parameters are listed in **Table 1**.

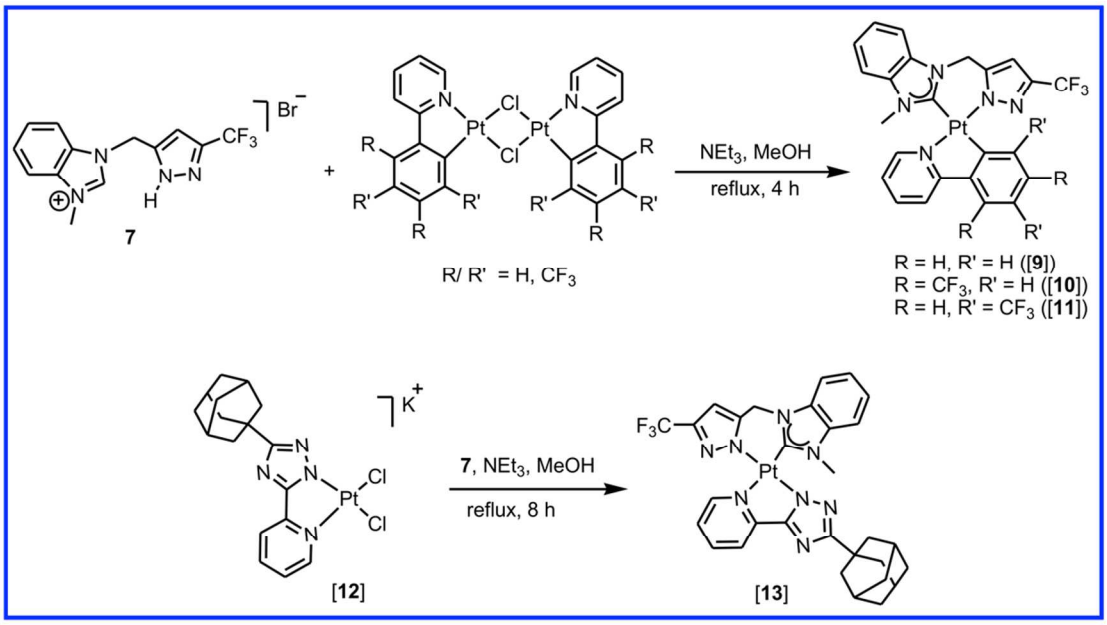

Scheme 2. Synthesis of Pt(II)-NHC complexes bearing phenyl-pyridine / triazole-pyridine chromophores.

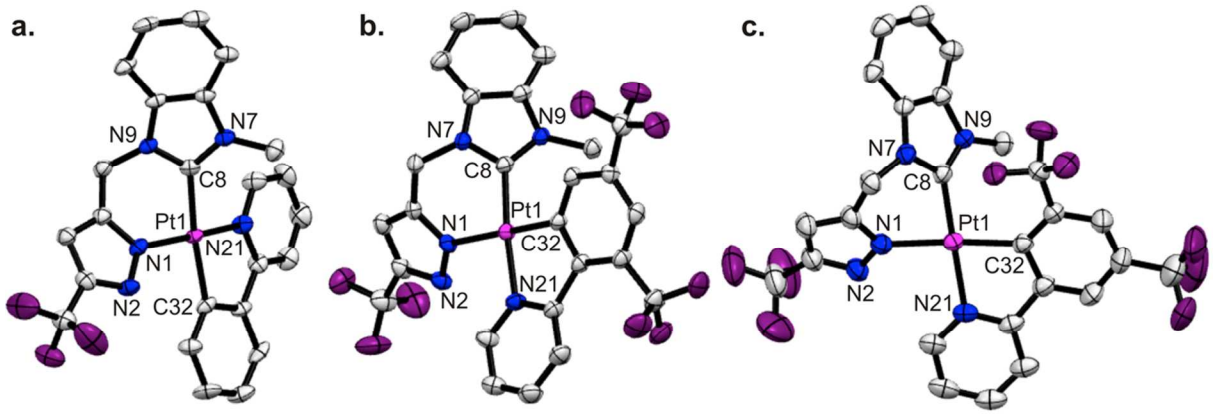

Figure 1. Structures obtained by X-ray diffractometry of [**9**] (a), [**10**] (b), and [**11**] (c) shown as 50% displacement ellipsoids (hydrogen atoms omitted for clarity).

The phenyl-pyridine–*N* and the carbenoid carbon of [**9**] adopt a *cis*- configuration, as opposed to [**10**] and [**11**] that display a *trans* configuration in order to avoid steric repulsion between the CF_3 groups of the pyrazole ring and the phenyl-pyridine-ligand. Due to the resulting *trans* labilizing effect of NHC ligands, the Pt–$N_{pyridine}$ bond distances in [**10**] and [**11**] are elongated as compared to that of [**9**]. The longer Pt–C_{NHC} bond distance observed in [**9**] (2.045(8) Å), as compared to those of [**10**] (1.981(4) Å) or [**11**] (1.967(4) Å), can be attributed to the *trans* disposed phenyl-*C* donor.

Table 1. Some relevant bonding parameters of complexes [**9**], [**10**] and [**11**]

Bond lengths (Å) /angles (deg)	[**9**]	[**10**]	[**11**]
Pt–C_{NHC}	2.045(8)	1.981(3)	1.967(4)
Pt–C_{Ph}	2.054(8)	1.991(3)	2.028(4)
Pt–$N_{Pyrazole}$	2.021(7)	2.100(3)	2.073(3)
Pt–$N_{Pyridine}$	2.026(7)	2.061(3)	2.073(3)
C_{NHC}–Pt–$N_{Pyrazole}$	84.8(3)	85.04(13)	83.37(15)
C_{NHC}–Pt–C_{Ph}	173.0(3)	96.82(14)	100.05(16)
C_{Ph}–Pt–$N_{Pyrazole}$	97.9(3)	175.05(13)	175.08(15)
$N_{Pyridine}$–Pt–$N_{Pyrazole}$	171.0(3)	98.62(12)	96.33(15)
$N_{Pyridine}$–Pt–C_{Ph}	81.0(3)	79.86(13)	80.78(16)
(N–C–N)NHC	107.0(7)	107.0(3)	106.6(4)

The bite angles of the bidentate NHC^pyrazolate ligands coordinated to the platinum centers (84.8(3)°, 85.04(13)° and 83.37(15)° in [**9**], [**10**] and [**11**] respectively) indicate a distorted square-planar configuration. Also in [**9**], the *trans* angles between the pyridyl fragment of the phenyl pyridine

ligand and the pyrazole fragment of the NHC-pyrazolate ligand clearly deviates from linearity (171.0(3)°). Similarly, in [**10**] and [**11**] the C_{ph} and the $N_{pyrazole}$ donor atoms occurring in *trans* configuration also feature platinum-centered *trans*-bond angles (C_{Ph}–Pt–$N_{pyrazole}$) of 175.05(13)° and 175.08(15)°, respectively. The inter-ligand bond angles ($N_{pyrazole}$–Pt–$N_{pyridine}$) in [**10**] and [**11**] were 98.62(12)° and 96.33(15)°, respectively.

Complex [**13**] also adopts a *trans* configuration between the $N_{pyridyl}$ atom and the C_{NHC} atom of the two bidentate ligands in order to avoid the steric repulsion between the bulky adamantyl group and the CF_3 substituent. As single crystals suitable for X-ray studies could not be obtained for complex [**13**], the bond connectivity and the geometry were established with the aid of 2D NMR spectroscopy (HMBC, HSQC and NOESY). Absence of polarization transfer within NHC methyl wingtip and the pyridyl-α_H protons of the complex [**13**] in the NOESY spectra confirms a *trans* configuration between these fragments.

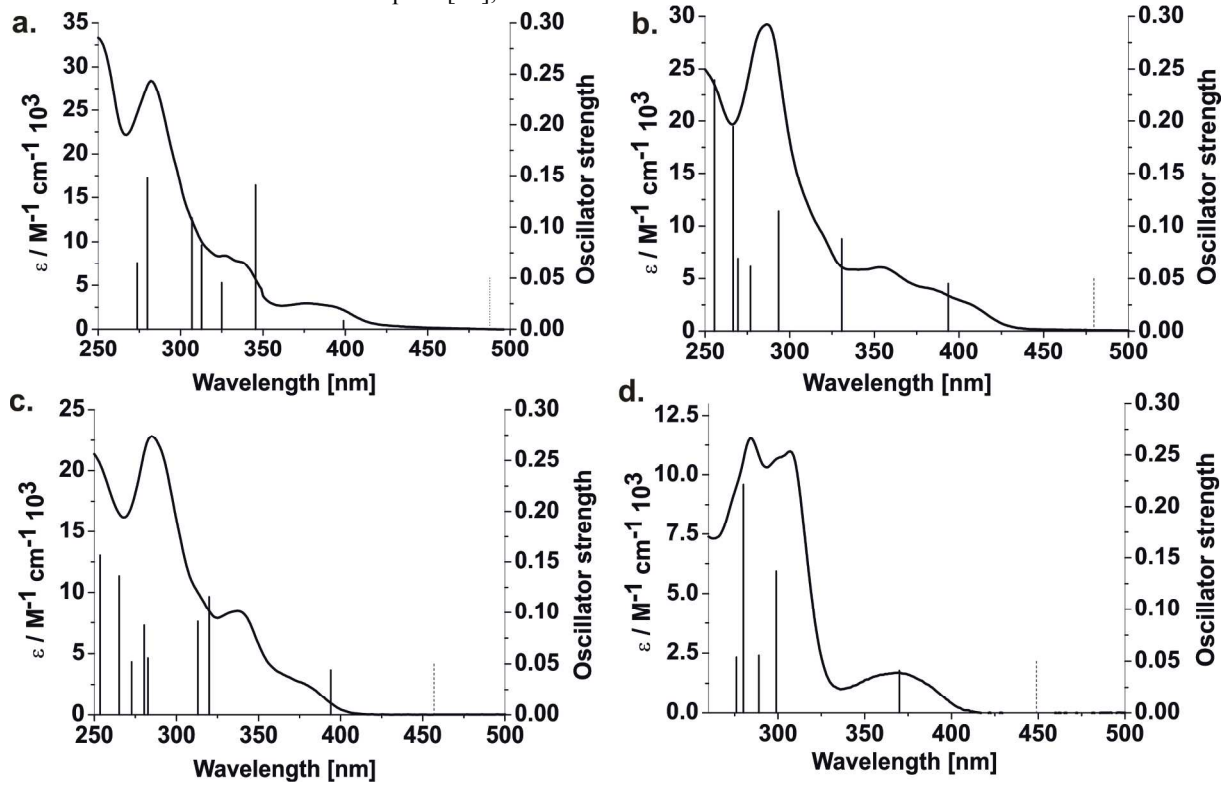

Figure 2. Absorption spectra and calculated transitions for complexes [**9**], [**10**], [**11**], [**13**] depicted in **a**, **b**, **c**, and **d**, respectively. The dashed lines represent the spin-forbidden S_0-T_1 transitions.

theory (TD-DFT). In addition quantum-chemical calculation were performed to predict the nature and energies of the main transitions. Isodensity surface plots of the highest occupied (HOMOs) and lowest unoccupied molecular orbitals (LUMOs), along with the energies of selected molecular frontier orbitals, are listed in tables **S1** and **S2** (ESI). The computed vertical transitions in vacuum, their oscillator strengths and the expansion coefficients of the corresponding monoelectronic excitations are listed in **Table S3**.

TD-DFT calculations reveal that the $S_0 \rightarrow S_1$ transitions for all complexes can be mainly described as HOMO→LUMO excitations, whereas higher energy transitions involve admixtures of HOMO–*n* and LUMO+*m* excitations. Complex [**9**] exhibits a platinum-centred HOMO orbital with significant contributions from the phenyl fragment of the cyclometalated-C^N ligand, whereas the LUMO (π^*) appears largely delocalized over the pyridyl fragment of the cyclometalated

Absorption spectroscopy and frontier orbitals

Absorption spectra of all complexes were measured in dichloromethane at ambient temperature and are depicted in **Figure 2**. In the figure are also shown the relevant electronic transitions calculated using time dependence density functional

C^N chelate with a small contribution from the phenyl ring as well as from the metal center. Hence, we reasonably ascribe the relatively weak band at 382 nm (HOMO→LUMO excitation) to an electronic transition with mixed intraligand charge-transfer (^{1}ILCT) and metal-to-ligand charge-transfer (^{1}MLCT) character.[28] The moderately intense absorption peak at relatively high energy (338 nm) is due to a HOMO–1→LUMO excitation, whereas the highest intensity absorption peak at 282 nm is due to an admixture of HOMO–5→LUMO and HOMO–1→LUMO+1 excitations. Orbital diagrams of both HOMO–1 and HOMO–5 orbitals show electron delocalization over the phenyl ring and the pyrazole/ benzimidazole fragments of the heteroleptic complex. As a sizeable participation of platinum-dπ orbitals is also observed in the HOMO–5, the HOMO–1 and the LUMO orbitals, we ascribe these electronic transitions peaking at 338 nm and 282 nm to mixed metal-

perturbed intra-ligand (^{1}ILCT)/ligand-to-ligand charge transfer (^{1}LLCT) transitions.

Frontier orbitals of complexes [**10**] and [**11**] display similar iso-surfaces. Analogously to [**9**], the LUMO remains primarily localized on the pyridyl fragment. However, the HOMO is spread over the phenyl rings of the cyclometalated C^N ligand and the pyrazole fragment of the chelating NHC^pyrazolate ligand. The orbital analysis indicates that the low energy absorption bands at 408 nm for [**10**] and at 381 nm for [**11**] can be ascribed to HOMO→LUMO transitions, whereas the intense absorption bands at higher energies (around 300 nm) are assigned to mixed metal-perturbed ^{1}ILCT/^{1}LLCT transitions arising from HOMO–4→LUMO for [**10**] and HOMO–1→LUMO / HOMO→LUMO+1 excitations for [**11**].

The HOMO of complex [**13**] is mainly localized on the triazole moiety. Analogously to the other complexes described herein, the LUMO appears pyridine-centered (π^*), but with significant contribution from Pt–dπ-orbitals. The low-energy absorption band peaking at 369 nm involves a HOMO→LUMO excitation and is ascribed to a mixed ^{1}MLCT/^{1}ILCT transition. The absorption bands at 306 nm and 282 nm are due to HOMO–1→LUMO and HOMO→LUMO+2 excitations, respectively, and can be ascribed to metal-perturbed ^{1}LLCT transitions.

All of the complexes were further characterized by cyclic voltammetry (CV) and differential pulse voltammetry (DPV), (**Table 2**, **Figure S6**). Each compound displays an irreversible oxidation wave in the range between +1.33 and +1.69 V, that can be attributed to HOMO-centred oxidation processes that clearly involve the metal centre. In particular a relatively facile oxidative process was observed for [**9**] (+1.33 V), in comparison to those of [**10**] (+1.64 V) and [**11**] (+1.69 V). The observed positive shift in the oxidation potential of [**10**] and [**11**] can be attributed to the presence of two additional electron withdrawing CF_3 groups in the bidentate ligand. In the range of −2.12 V to −1.62 V, complexes [**9**], [**11**] and [**13**] display irreversible reduction processes, whereas complex [**10**] reveals a quasi-reversible behaviour (ΔE_p = 0.11 mV). Such reduction processes are pyridine-centered,[10b] as also suggested by the calculated unoccupied frontier orbitals. The reduction potentials of [**10**] and [**11**] are, as expected, less negative than that of [**9**], due to the presence of the electron withdrawing CF_3 groups on the ligands and are −1.62 V and −1.91 V, respectively (see table 2). ~~The observed trend in the electrochemical HOMO–LUMO gaps also correlate well with the one observed on the emission spectra (*vide infra*)~~. However, it is clear that the emissive excited states cannot be described as pure HOMO-LUMO excitations, as also indicated by the TD-DFT calculations (*vide supra*).

Table 2. Electrochemical data of complexes [**9**], [**10**], [**11**], and [**13**]. The potentials are given *vs* SCE., saturated calomel electrode (SCE). [a]

Complex	E_{pa} (HOMO)	E_{pc} (LUMO)	$\Delta E_{HOMO-LUMO}$ (eV)
[**9**]	1.33 V (−5.92 eV)	–2.12 V (–2.97 eV)	2.95
[**10**]	1.64 V (−6.17 eV)	–1.62 V (–3.31 eV)	2.86
[**11**]	1.69 V (−6.29 eV)	–1.91 V (–3.05 eV)	3.24
[**13**]	1.65 V (−6.31 eV)	–1.97 V (–3.10 eV)	3.21

[a] 1 mM of each complex in dichloromethane solution in the presence of 0.1 M $TBAPF_6$, glassy carbon 3 mm, ν = 0.1 Vs^{-1}. [b] The HOMO and LUMO energies were calculated using the relation: $E_{HOMO/LUMO} = -(E_{onset\ ox./red.}$ vs $Fc/Fc^+ + 4.8)$ (eV).[29]

Photophysical characterization

Emission spectra of complexes [**9**], [**10**], [**11**], [**13**] at ambient temperature and at 77 K are depicted in **Figure 3** (the corresponding excitation spectra are shown in **Figures S1**–**S4**). Thin film emission spectra of [**9**], [**10**], [**11**], [**13**] are depicted in **Figure 4** (10% wt doped into PMMA) and **Figure S5** (neat films). **Table 3** summarizes all relevant photophysical data in solution and in glassy matrices at 77 K, whereas **Table 4** includes the data for the films.

Table 3. Photophysical data in solution.

complex	λ_{abs} [nm] (ε x 10^{-3} / [$M^{-1}cm^{-1}$]) [a],[b]	λ_{em} (rt) [nm] [a],[c]	λ_{em} (77K) [nm] [d]	Φ_{em} (x100, aer.) [a],[e]	Φ_{em} (x100, deaer.) [a],[e]	τ (rt, aer.) [µs] [a]	τ (rt, deaer.) [µs] [a]	τ (77 K) [µs] [c]	$k_r \times 10^{-4}$ [s^{-1}]	$k_{nr} \times 10^{-5}$ [s^{-1}]
[**9**]	282 (28.4) 338 (7.5) 382 (2.7)	487 518	482 518	0.2	0.7	0.004 (33%) 0.070 (67%)	0.9 (45%) 8.2 (55%)	12.2	0.14	2.0
[**10**]	288 (29.5) 354 (6.1) 408 (2.7)	547	508 547	1.0	1.5	0.41	1.0 (77%) 12.4 (23%)	11.9	0.41	2.7
[**11**]	286 (22.6) 338 (8.2) 381 (2.1)	489 519	481 515	5.0	8.0	0.1	1.3 (70%) 16.4 (30%)	20.7	1.4	1.6
[**13**]	282 (11.3) 306 (8.4) 369 (1.8)	476 505	461 492	1.5	7.2	0.36	2.6	19.8	2.7	3.5

[a] In dichloromethane solution. [b] The abbreviation "sh" denotes a shoulder [c] λ_{exc} = 282 nm ([**9**]), 354 nm ([**10**]), 284 nm ([**11**]), 285 nm [**13**]. [d] In a 2-MeTHF glassy matrix. [e] Quantum yields were measured with an integrating sphere.

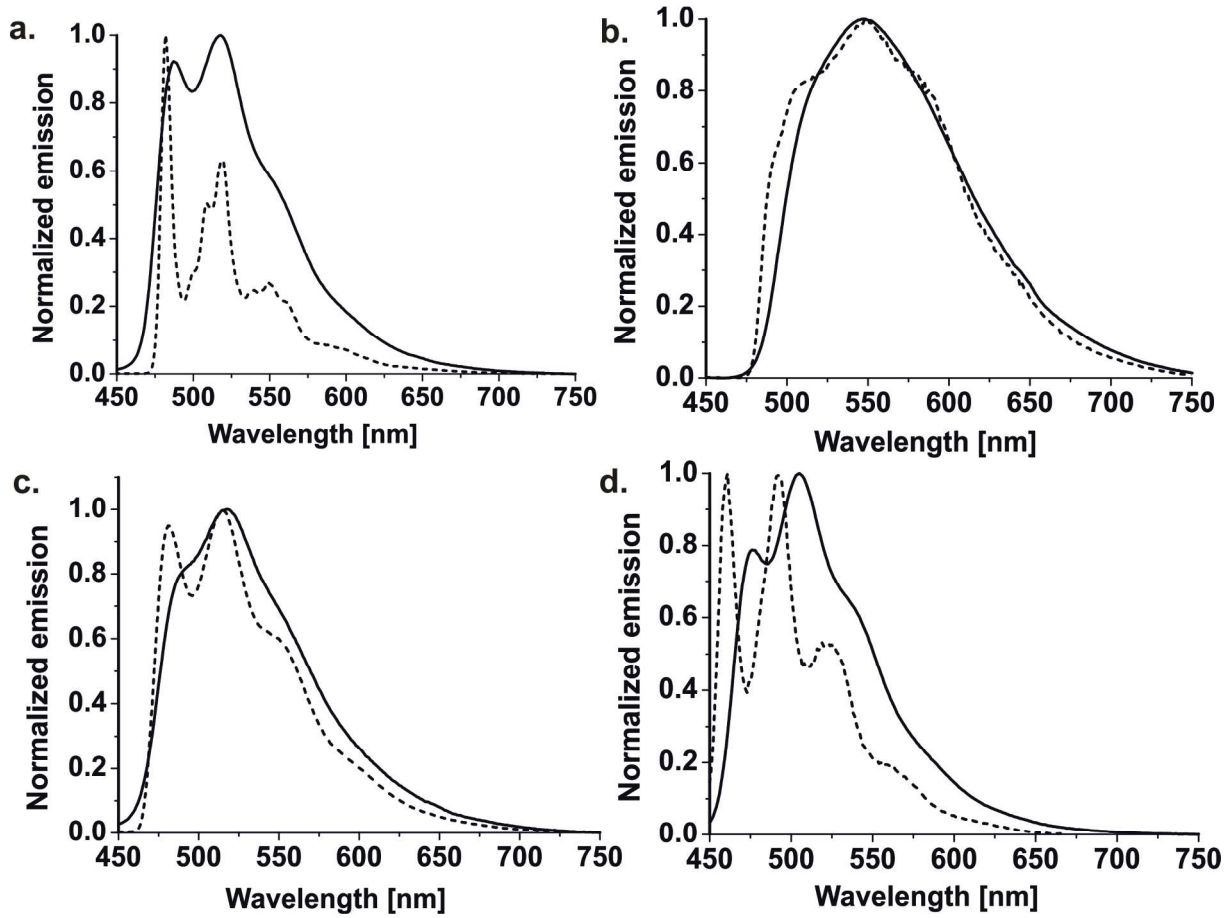

Figure 3. Emission spectra of complexes [**9**] (a), [**10**] (b), [**11**] (c), [**13**] (d) at ambient temperature (solid lines) and 77 K (dashed lines). Excitation wavelengths: 357 nm, 354 nm, 336 nm and 308 nm, respectively.

Table 4. Photophysical data in films.

Complex	λ_{em} (neat film) [nm][a],[b]	λ_{em} (10 % wt in PMMA) [nm][a]	Φ_{em} (x100, neat film)[a],[c]	Φ_{em} (x100, 10% wt in PMMA)[a],[c]	τ (neat film) [μs]	τ (10% wt in PMMA) [μs]	$k_r \times 10^{-4}$ [s^{-1}][d]	$k_{nr} \times 10^{-4}$ [s^{-1}][d]
[**9**]	491 527	489 524	3.4	34.0	0.7 (65%) 12.8 (35%)	14.1	2.4	4.6
[**10**]	518 543	509 537	10.0	26.7	9.9	4.0 (38%) 15.9 (63%)	2.3	6.4
[**11**]	494 521	490 518	3.2	10.0	2.6 (41%) 11.1 (59%)	3.1 (16%) 16.1 (84%)	0.7	6.4
[**13**]	474 501	470 498 537 (sh)	11.0	49.0	3.7 (54%) 14.6 (46%)	18.8	2.6	2.7

[a] λ_{exc} = 357 nm ([**9**]), 354 nm ([**10**]), 336 nm ([**11**]), 308 nm [**13**]. [b] The abbreviation "sh" denotes a shoulder [c] Quantum yields were measured in an integrating sphere system [d] 10% wt in PMMA.

In fluid dichloromethane at room temperature, [**9**] and [**11**] display comparable luminescence spectra. Complex [**9**] emits with a clear vibrational progression typical for predominantly ligand-centered states, with a maximum at 487 nm. The emission profile of complex [**11**] has a less pronounced band at 489 nm and a maximum at 519 nm. A remarkable characteristic of complex [**10**] is its featureless and broad emission, which appears with a large bathochromic shift as compared to [**9**] and [**11**]. This smaller energy gap of [**10**], if compared with complex [**11**], is a result of the CF_3-substitution pattern, as the *m,m´*-substitution lowers the π^*-orbital energy of the C^N ligand to a larger extend than for the *o,p*-pattern. Indeed, the calculated MO energies reveal that the position of the CF_3 substituents mostly affects the LUMO without significantly altering the HOMO of the complexes. The bluest emission is observed for complex [**13**] bearing the pyridine-triazole luminophore. Its emission spectrum in dichloromethane peaks at 476 nm and at 505 nm. The sensitivity of the long excited state lifetimes towards oxygen is indicative of emissions from the triplet manifolds.

In glassy matrices of 2-MeTHF at 77 K the emission spectra of [**9**] and [**11**] display enhanced vibrational progressions which are indicative of a predominant LC character. In contrast, the emission spectrum of [**10**] remains essentially unaffected. A hypsochromic shift with a pronounced vibrational progression was observed for complex [**13**] at 77K, and is most likely caused by a loss of MLCT character in the frozen environment.

The photoluminescence quantum yields in solutions are relatively low for all complexes, even in deaerated conditions, which is due to solvent-related vibronic deactivation of the excited states. Indeed, a significant enhancement of the solid state PLQY is observed in 10% wt doped PMMA films, where complex [**13**] reaches up to 49 % (**Table 4**).

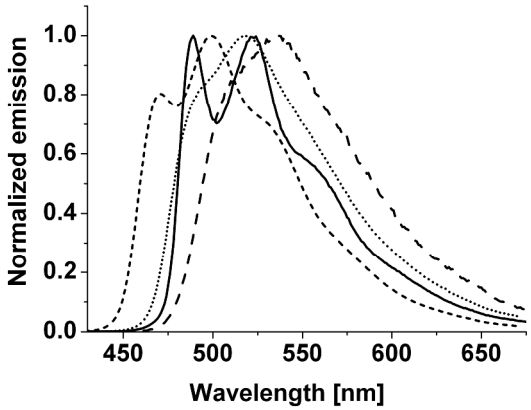

Figure 4. Emission spectra of [**9**] (solid line), [**10**] (long dashed line), [**11**] (dotted line) and [**13**] (short dashed), in 10% wt PMMA films. Excitation wavelengths: 357 nm, 354 nm, 336 nm and 308 nm respectively.

Conclusions

In summary, we have synthesized a new bidentate NHC^pyrazolate ligand precursor featuring a methylene spacer between the benzimidazole-2-ylidene and the pyrazolate moieties. It was used to obtain four new luminescent platinum(II) complexes along with either phenyl-pyridine or pyridine-triazole luminophores. A full structural, electrochemical and photophysical characterization was carried out, and the results interpreted with the aid of TD-DFT calculations. Emission of the complexes were in the sky blue/green region of the electromagnetic spectrum. Amongst all the complexes reported herein, the one featuring a pyridine-triazole luminophore along with the bidentate NHC^pyrazolate ligand exhibited a more blue phosphorescence with high photoluminescence quantum yield in the solid state. Additional tweaking of the pyridine-triazole chromophore (for instance, replacing then adamantyl moiety by a CF_3 group) could further shift the emission into the blue, as the HOMO would be stabilized and the HOMO-LUMO gap would be increased, along with the energy of the emissive triplet state. Thus, the new bidentate building block introduced herein constitutes a convenient tool in the design of phosphorescent metal complexes for optoelectronic applications if combined with a suitable luminophore.

Experimental

Synthetic methods and characterization

All reagents were of analytical grade and used as received. Solvents were purified according to standard procedures. All reactions were performed under an atmosphere of nitrogen using standard Schlenk techniques unless specified otherwise. Column chromatography was performed using silica gel 60 (particle size 63–200 mm or 230–400 mesh, Merck). NMR spectra were recorded either on a Bruker AV 300/400 or an Agilent DD2 600 MHZ spectrometer. All chemical shifts are given in ppm and referenced to the residual solvent peaks. ^{19}F NMR are referenced to $CFCl_3$ (0.00 ppm) as an internal standard. The signals are abbreviated as follows: s, singlet; d, doublet; t, triplet; q, quartet; m, multiplet. All coupling constants (*J*) are given in Hertz (Hz). High resolution Mass Spectra (HRMS) of all complexes were measured at the department of Organic Chemistry, University of Muenster in a Bruker Daltronics or Micro TOF with loop injection. Elemental analyses were recorded at University of Münster, Germany or at the University of Milano, Italy.

Photophyscis.

Absorption spectra were measured on a Varian Cary 5000 double-beam UV-Vis-NIR spectrometer and baseline corrected. Steady-state emission spectra were recorded on a Horiba Jobin–Yvon IBH FL-322 Fluorolog 3 spectrometer equipped with a 450 W xenon-arc lamp, double grating excitation, and emission monochromator (2.1 nm mm^{-1} of dispersion), and a Hamamatsu R928 photomultiplier tube or a TBX-4-X single photon-counting detector. Emission and excitation spectra were corrected for source intensity (lamp and grating) by standard

correction curves. Time-resolved measurements were performed using the time-correlated single-photon counting (TCSPC) option on the Fluorolog 3 equipment. NanoLEDs (295 nm; full width at half maximum, 1 ns) with repetition rates between 10 kHz and 1 MHz were used to excite the sample. The excitation sources were mounted directly on the sample chamber at 90° to a double-grating emission monochromator (2.1 nm mm^{-1} of dispersion, 1200 $grooves^{-1}$) and collected by a TBX-4-X single photon counting detector. The photons collected at the detector were correlated by means of time to amplitude converter to excitation pulse. Signals were collected with the aid of IBH Data-station Hub photon counting module and data analysis was performed by using DAS6 program (Horiba Jobin–Yvon IBH). The quality of the fit was assessed by minimizing the reduced χ^2 function and visually inspecting the weighted residuals. Luminescence quantum yields were measured with a Hamamatsu Photonics absolute PL quantum yield measurement system (C9920-02) equipped with a L9799-01 CW Xenon light source (150 W), monochromator, C7473 photonic multi-channel analyser, integrating sphere and employing U6039-05 PLQY measurement software (Hamamatsu Photonics Ltd., Shizuoka, Japan). All solvents used were of spectrometric grade. Deaerated samples were prepared by the freeze-pump-thaw-technique.

Computational Details.

Geometries were optimized by means of density functional theory (DFT). The parameter-free hybrid functional Perdew Burke Ernzerhof[30] was employed along with the standard valence double-ζ polarized basis set 6-31G(d,p)[31] for C, H, F and N. For Pt, the Stuttgart_Dresden (SDD) effective core potentials were employed along with the corresponding valence triple-ζ basis set. No imaginary frequency was obtained (NImag = 0). Simulated electronic absorption spectra were computed on the optimized geometry at S_0 by means of time-dependent density functional theory (TD-DFT) calculations.[32] All the calculations were performed for vacuum conditions using the Gaussian 09 program package.[33]

Cyclic Voltammetry.

All photoactive complexes reported herein are characterized by cyclicvoltammetry (CV) and differential pulse voltammetry (DPV) in dichloromethane solution and in presence of tetra-*n*butylammonium hexafluorophosphate ($TBAPF_6$, 0.1 M) as supporting electrolyte. The concentration of the all samples was 1 mM in dichloromethane (Sigma-Aldrich, Chromasolv® Plus, 99.9 %). $TBAPF_6$ (electrochemical grade, 99%, Fluka) was used as the supporting electrolyte. The solvent and the supporting electrolyte were used as received without any further purification. For the electrochemical experiments, a CHI750C electrochemical workstation (CH Instruments, Inc., Austin, TX) was used. Electrochemical experiments were performed in a glass cell under an argon atmosphere. To minimize the Ohmic drop between the working and the reference electrodes, the feedback correction was employed. A 3 mm diameter glassy carbon disk electrode (CH Instruments, Inc., Austin, TX) was employed as the working electrode. The working electrode was polished with a 0.05 μm diamond suspension (Metadi Supreme Diamond Suspension, Buehler) before each measurement. A platinum wire served as a counter electrode, while a silver wire was employed as a quasi-reference electrode (Ag-QRE), which was separated from the cathode by a glass frit (Vycor). The reference electrode was calibrated at the end of each experiment against the ferrocene/ferricenium couple (Fc/Fc^+), whose formal potential against the saturated calomel electrode (SCE) was 0.46 V in dichloromethane; all potential values are reported against the SCE.

X-Ray diffraction.

Data sets were collected with a Nonius KappaCCD diffractometer. Programs used: data collection, COLLECT (Nonius B.V., 1998); data reduction Denzo-SMN;[34] absorption correction;[35] structure solution SHELXS-97;[36] structure refinement SHELXL-97[37] and graphics, XP (BrukerAXS, 2000). Thermals ellipsoids are shown with 50% probability. *R*-values are given for observed reflections, and wR^2 values are given for all reflections (See supporting information for crystallographic data).

Syntheses

Compound 7.
1-methyl benzimidazole (235.1 mg, 1.78 mmol) was added to a solution of compound **6** (408 mg, 1.78 mmol) in dichloromethane (20 mL) and heated under reflux for 4 h. Precipitation of a colourless solid was observed, upon completion of this time. The dichloromethane solution was further concentrated to half the volume (≈ 10 mL) to ensure complete precipitation. The resultant precipitate was filtered and washed again with dry diethyl ether (20 mL × 3) using a filter-cannula under an atmosphere of N_2 to avoid the contact with moisture. Upon drying the colourless solids *in vacuo*, an analytically pure form of the ligand precursor **7** was isolated as hygroscopic powder. Yield: 686 mg (88.2%). ^{1}H NMR (300 MHz, DMSO-d_6): δ 14.33 (s, 1H, Pyrazole N*H*), 9.93 (s, 1H, C_2-H), 8.05 (d, J = 3.66 Hz, 2H, benzimidazole-H), 7.70 (d, J = 3.66 Hz, 2H, benzimidazole-H), 6.94 (s, 1H, pyrazole-H), 5.95 (s, 2H, methylene bridge), 4.11 (s, 3H, CH_3). ^{13}C{^{1}H} NMR (101 MHz, CD_2Cl_2): δ 154.3, 143.3, 137.0, 131.9, 130.5, 127.4, 126.8, 126.6, 113.8, 113.3, 104.3, 48.3 (–(*C*H$_2$)–), 33.5 (*C*H$_3$). ^{19}F NMR (282 MHz, DMSO-d_6): δ −60.42. MS (ESI HRMS) *m/z* (%): 281.1010 (100) [**7**]$^+$, (calcd. for [**7**]$^+$ 281.1009).

Compound 8. (2-(3-(adamantan-1-yl)-1*H*-1,2,4-triazol-5-yl)pyridine).
This ligand precursor was prepared according to a previously known procedure, using adamantane-carbonylchloride.[26] Yield: 1.3 g, (91.0%). ^{1}H NMR (300 MHz, $CDCl_3$) δ 8.69 (d, J = 4.0 Hz, 1H), 8.20 (d, J = 7.9 Hz, 1H), 7.81 (t, J = 7.0 Hz, 1H), 7.41–7.29 (m, 1H), 2.12 (s, 9H), 1.81 (s, 6H). MS (ESI HRMS) (*m/z*): 281.1762 [**8**+H]$^+$, (calcd. for [**8**+H]$^+$ 281.1761), 303.1580 [**8**+Na]$^+$, (calcd. for [**8**+Na]$^+$ 303.1580).

COMPOUND [9] (R = H).

A mixture of the ligand precursor **7** (100 mg, 0.27 mmol), platinum(II)–phenylpyridine dimer (R = H) (106 mg, 0.14 mmol) and triethylamine (109 mg, 1.08 mmol) was dissolved in methanol (10 mL) in a flame-dried schlenk flask. The reaction mixture was heated under refluxion for 6 h. After this time, the solvent was removed *in vacuo* and the product was suspended in dichloromethane and washed with water (1:1, *V*:*V*). The organic phase was separated and dried over $MgSO_4$ and dichloromethane was removed *in vacuo*. Further purification of the crude product was done on a silica gel column using a mixture of dichloromethane: methanol (10:1, *V*:*V*) as eluent to obtain [**9**] as pale yellow powder. Yield: 46 mg (27.1%). ^{1}H NMR (300 MHz, CD_2Cl_2): δ 10.01 (ddd, J = 5.8 Hz, 1.6 Hz, 0.8 Hz, 1H), 8.53 (m, 1H), 8.31 (m, 1H), 7.86 (m, 2H), 7.65 (dd, J = 7.7 Hz, 1.2 Hz, 1H), 7.60 (m, 1H), 7.44 (m, 2H), 7.34 (td, J = 7.4 Hz, 1.3 Hz, 1H), 7.18 (td, J = 7.4 Hz, 1.4 Hz, 1H), 7.01 (ddd, J = 7.4 Hz, 5.9 Hz, 1.7 Hz, 1H), 6.49 (s, 1H), 5.43 (s, 1H), 5.30 (s, 1H), 3.91 (s, 3H). ^{13}C{^{1}H} NMR (101 MHz, CD_2Cl_2): δ 168.7, 157.7, 151.9, 150.2, 146.8, 142.9, 139.9, 138.4, 137.2, 135.6, 130.4, 129.3, 127.3, 124.2, 123.9, 123.0, 122.7, 120.9, 119.0, 111.6, 110.5, 101.4 (d, J = 2.1 Hz), 44.3 (–(*C*H$_2$)–), 36.4 (*C*H$_3$). ^{19}F NMR (282 MHz, CD_2Cl_2): δ −60.52. MS (ESI HRMS) *m/z* (%): 629.12201 (100) [**9**+H]$^+$, (*calcd. for* [**9**+H]$^+$ 629.1235). *Anal. Calcd.* (for $C_{24}H_{19}F_3N_5Pt{\cdot}H_2O{\cdot}$hexanes): C, 49.31; H, 4.41; N, 9.58. *Found:* C, 49.56; H, 4.48; N, 9.65.

COMPOUND [10] (R = *o*,*p*-CF_3).

A mixture of the ligand precursor **7** (100 mg, 0.27 mmol), platinum(II)–phenyl pyridine dimer (R = *o*,*p*-CF_3) (145 mg, 0.14 mmol) and triethylamine (109 mg, 1.08 mmol) was dissolved in methanol (10 mL) in a flame-dried schlenk flask and heated under refluxion for 6 h. Subsequent work-up procedure was analogous to that of compound [**9**]. Further purification of the crude product was done by silica gel column chromatography using a mixture of dichloromethane: methanol (*V*: *V*, 10:0.5) to obtain [**10**] as crystalline yellow solid. Yield: 92 mg (44.4%). ^{1}H NMR (400 MHz, CD_2Cl_2): δ 10.22 (ddd, J = 5.7 Hz, 1.7 Hz, 0.7 Hz, 1H), 8.29 (d, J = 8.5 Hz, 1H), 8.06 (ddd, J = 8.5 Hz, 7.5 Hz, 1.8 Hz, 1H), 7.79 (m, 1H), 7.65 (m, 2H), 7.53 (m, 2H), 7.45 (m, 2H), 6.57 (s, 1H), 5.41 (s, 1H), 5.39 (s, 1H), 3.93 (s, 3H). ^{13}C{^{1}H} NMR (101 MHz, CD_2Cl_2) δ 166.5 (C_{NHC}), 161.4, 154.0, 152.0, 150.2, 148.6, 142.1, 141.7, 138.8, 136.8, 136.3, 135.4, 134.1, 132.8, 131.8, 128.7, 123.5, 123.4 (d, J = 10.4 Hz), 123.1, 122.4, 118.9, 110.4, 109.4, 100.4 (d, J = 1.8 Hz), 43.0 (–(*C*H$_2$)–), 34.8 (*C*H$_3$). ^{19}F NMR (282 MHz, CD_2Cl_2): δ −57.36 (s, satellites were observed with J = 13.0 Hz), −60.49 (s, satellites were observed with J = 36.0 Hz), −63.16 (s). MS (ESI HRMS) *m/z* (%): 765.0988 (100) [**10**+H]$^+$, (*calcd. for* [**10**+H]$^+$ 765.0985). *Anal. Calcd.* (for $C_{26}H_{16}F_9N_5Pt$): C, 40.84; H, 2.11; N, 9.16. *Found:* C, 40.79; H, 2.26; N, 9.23.

COMPOUND [11] (R = *mm*' CF_3).

A mixture of the ligand precursor **7** (100 mg, 0.27 mmol), platinum(II)–phenylpyridine dimer (R = *m*, *m*'-CF_3) (145 mg, 0.14 mmol) and triethylamine (109 mg, 1.08 mmol) was dissolved in methanol (10 mL) in a flame-dried schlenk flask and heated under refluxion for 6 h. Work-up procedure analogous to that of compound [**9**] was followed to obtain crude sample. Further purification of the crude was done on a silica gel column using dichloromethane: methanol (10:0.5, *V*: *V*) as eluent to obtain [**11**] as pale yellow powder. Yield: 52 mg (25.2%). ^{1}H NMR (300 MHz, CD_2Cl_2): δ 9.73 (ddd, J = 5.7 Hz, 1.6 Hz, 0.8 Hz, 1H), 8.08 (t, J = 1.2 Hz, 1H), 8.00 (dd, J = 1.5 Hz, 0.8 Hz, 1H), 7.70 (s 1H), 7.61 (d, J = 8.02 Hz, 1H), 7.47 (ddd, J = 7.3, 5.7, 1.5 Hz, 1H), 7.37 (m, 4H), 7.35 (m, 1H), 6.56 (s, 1H), 5.48 (s, 1H), 5.41 (s, 1H), 3.56 (s, 3H). ^{13}C{^{1}H} NMR (75 MHz, CD_2Cl_2): δ 166.0 (C_{NHC}), 164.5, 160.7, 152.4, 150.3, 143.6, 140.2, 138.0, 137.6, 135.0, 134.4, 133.9, 130.2, 126.9, 126.4, 124.3, 124.0, 123.6, 122.4, 121.8, 119.8, 113.3, 110.6, 101.6 (d, J = 2.1 Hz, pyrazole-*C*), 44.2 (–(*C*H$_2$)–), 35.4 (*C*H$_3$). ^{19}F NMR (282 MHz, CD_2Cl_2): δ −62.85, −60.61, −58.63. MS (ESI HRMS) *m/z* (%): 765.0992 (100) [**11**+H]$^+$, (*calcd. for* [**11**+H]$^+$ 765.0985). *Anal. Calcd.* (for $C_{26}H_{16}F_9N_5Pt$): C, 40.84; H, 2.11; N, 9.16. *Found:* C, 40.57; H, 2.47; N, 8.33.

COMPOUND [12] (Potassium dichloro(pyridine-triazole^{Ad}) platinate).

To a solution of 2-(3-(adamantan-1-yl)-1*H*-1,2,4-triazol-5-yl)pyridine (140 mg, 0.5 mmol) in methoxyethanol (25 mL) was added a solution of K_2PtCl_4 (208 mg, 0.5 mmol) in water (10 mL) and reaction mixture was stirred at 85 °C overnight. After cooling the reaction mixture to ambient temperature, the yellow precipitate was filtered off, washed with water, ethanol and diethylether and finally dried *in vacuo*. Yield: 185 mg (68.0 %). ^{1}H NMR (300 MHz, DMF-*d7*) δ 9.55 (d, J = 5.8 Hz, 1H), 8.47 (t, J = 7.8 Hz, 1H), 8.25 (d, J = 7.9 Hz, 1H), 7.87 (td, J = 6.0 Hz, 2.9 Hz, 1H), 2.14 (s, 9H), 1.80 (s, 6H). ^{13}C{^{1}H} NMR spectra of this precursor complex could not be obtained due to its poor solubility in the DMF-d_7. MS (ESI HRMS, negative mode) *m/z* (%): 544.0641 (100) [**12**]$^-$, (*calcd. for* [**12**]$^-$ 544.0646). *Anal. Calcd.* (for $C_{24}H_{19}F_3N_5Pt$): C, 34.94; H, 3.28; N, 9.59. *Found*: C, 34.68; H, 3.37; N, 9.63.

COMPOUND [13]

A mixture of ligand precursor **7** (60 mg, 0.16 mmol), potassium dichloro(pyridine-triazole^{Ad})platinate (97 mg, 0.16 mmol) and triethylamine (100 mg, 0.98 mmol) in methanol (10 mL) in a flame-dried schlenk flask was heated under refluxion for 6 h. After completion of the reaction, solvents were dried *in vacuo* and the product was suspended in dichloromethane and washed with water(1:1, *V*: *V*). The organic phase was separated and dried over $MgSO_4$ and dichloromethane was removed *in vacuo*. Further purification was done using a preparative TLC with a mixture of dichloromethane: hexane (10:2, *V*: *V*) as eluent to obtain [**13**] as a colourless powder. Yield: 28 mg (23.1%). ^{1}H NMR (600 MHz, CD_2Cl_2): δ 9.73 (dt, J = 5.7 Hz, J = 1.2 Hz, 1H), 8.03–8.00 (m, 2H), 7.60–7.57 (m, 2H), 7.49–7.40 (m, 3H), 6.65 (s, 1H), 5.35 (d, J = 2.2 Hz, 2H), 4.21 (s, 3H), 2.04 (s, 6H), 1.79 (s, 3H), 1.27 (s, 6H). ^{13}C{^{1}H} NMR (151 MHz, CD_2Cl_2): δ 174.3 (C_{NHC}), 163.6 (triazole-*C*), 151.6 (pyridyl-*C*), 151.3 (pyridyl-*C*), 141.9 (s), 140.9 (pyrazole-*C*), 140.0 (pyridyl-*C*) 135.3 (benzimidazole-*C*), 135.1 (pyrazole-*C*), 134.2 (triazole-*C*), 133.7 (benzimidazole-*C*), 124.7 (benzimidazole-*C*), 124.4 (benzimidazole-*C*), 124.1 (pyridyl-*C*), 120.3 (pyridyl-*C*), 112.0 (benzimidazole-*C*), 110.6 (benzimidazole-*C*), 101.8 (d, J = 2.1 Hz, pyrazole-*C*), 44.0 (adamantyl-*C*), 42.6 (–(*C*H$_2$)–), 37.5 (*C*H$_3$), 36.7 (adamantyl-*C*), 29.4 (adamantyl-*C*). ^{19}F NMR (564 MHz, CD_2Cl_2): δ −60.89. MS (ESI HRMS) *m/z* (%): 754.2194 (100) [**13**+H]$^+$ (*calcd. for* [**13**+H]$^+$ 754.2101).

Acknowledgements

Funding from the Federal Ministry for Education and Research (BMBF-Germany, project So-Light) is gratefully acknowledged. Authors also acknowledge Dr. Heinrich Luftmann for the support in HRMS measurements. CGD acknowledges Dr. Roland Fröhlich for support in diffractometric measurements and data refinement.

Notes and references

1. (a) T. Bessho, S. M. Zakeeruddin, C. Y. Yeh, E. W. Diau and M. Gratzel, *Angew. Chem. Int. Ed.*, 2010, **49**, 6646-6649; (b) M. G. Lobello, K. L. Wu, M. A. Reddy, G. Marotta, M. Gratzel, M. K. Nazeeruddin, Y. Chi, M. Chandrasekharam, G. Vitillaro and F. De Angelis, *Dalton Trans.*, 2014, **43**, 2726-2732; (c) S. Mathew, A. Yella, P. Gao, R. Humphry-Baker, B. F. E. Curchod, N. Ashari-Astani, I. Tavernelli, U. Rothlisberger, M. K. Nazeeruddin and M. Gratzel, *Nature Chem*, 2014, **6**, 242-247; (d) A. Luechai, J. Gasiorowski, A. Petsom, H. Neugebauer, N. S. Sariciftci and P. Thamyongkit, *J. Mater. Chem.*, 2012, **22**, 23030-23037.
2. (a) E. Balaraman, C. Gunanathan, J. Zhang, L. J. Shimon and D. Milstein, *Nature Chem.*, 2011, **3**, 609-614; (b) C. Federsel, A. Boddien, R. Jackstell, R. Jennerjahn, P. J. Dyson, R. Scopelliti, G. Laurenczy and M. Beller, *Angew. Chem. Int. Ed.*, 2010, **49**, 9777-9780.
3. (a) M. A. Baldo, M. E. Thompson and S. R. Forrest, *Nature*, 2000, **403**, 750-753; (b) S. Lamansky, P. Djurovich, D. Murphy, F. Abdel-Razzaq, H.-E. Lee, C. Adachi, P. E. Burrows, S. R. Forrest and M. E. Thompson, *J. Am. Chem. Soc.*, 2001, **123**, 4304-4312; (c) H. Yersin, in *Highly Efficient OLEDs with Phosphorescent Materials*, Wiley-VCH Verlag GmbH & Co. KGaA, 2008, pp. I-XVIII; (d) M. K. Nazeeruddin, R. Humphry-Baker, D. Berner, S. Rivier, L. Zuppiroli and M. Graetzel, *J. Am. Chem. Soc.*, 2003, **125**, 8790-8797.
4. W. Y. Wong and C. L. Ho, *J. Mater. Chem.*, 2009, **19**, 4457-4482.
5. M. A. Baldo, C. Adachi and S. R. Forrest, *Phys. Rev. B* 2000, **62**, 10967-10977.
6. (a) N. Darmawan, C. H. Yang, M. Mauro, M. Raynal, S. Heun, J. Pan, H. Buchholz, P. Braunstein and L. De Cola, *Inorg. Chem.*, 2013, **52**, 10756-10765; (b) J. M. Fernandez-Hernandez, C. H. Yang, J. I. Beltran, V. Lemaur, F. Polo, R. Frohlich, J. Cornil and L. De Cola, *J. Am. Chem. Soc.*, 2011, **133**, 10543-10558; (c) C. H. Yang, J. Beltran, V. Lemaur, J. Cornil, D. Hartmann, W. Sarfert, R. Frohlich, C. Bizzarri and L. De Cola, *Inorg. Chem.*, 2010, **49**, 9891-9901; (d) M. Mydlak, C. Bizzarri, D. Hartmann, W. Sarfert, G. Schmid and L. De Cola, *Adv. Funct. Mater.*, 2010, **20**, 1812-1820; (e) C. E. Welby, L. Gilmartin, R. R. Marriott, A. Zahid, C. R. Rice, E. A. Gibson and P. I. Elliott, *Dalton Trans.*, 2013, **42**, 13527-13536; (f) F. Dumur, M. Lepeltier, B. Graff, E. Contal, G. Wantz, J. Lalevée, C. R. Mayer, D. Bertin and D. Gigmes, *Synthetic Metals*, 2013, **182**, 13-21.
7. (a) M. Duati, S. Fanni and J. G. Vos, *Inorg. Chem. Commun.*, 2000, **3**, 68-70; (b) M. Duati, S. Tasca, F. C. Lynch, H. Bohlen, J. G. Vos, S. Stagni and M. D. Ward, *Inorg. Chem.*, 2003, **42**, 8377-8384; (c) R. Hage, R. Prins, J. G. Haasnoot, J. Reedijk and J. G. Vos, *Dalton Trans.*, 1987, 1389.
8. M. Mauro, E. Q. Procopio, Y. H. Sun, C. H. Chien, D. Donghi, M. Panigati, P. Mercandelli, P. Mussini, G. D'Alfonso and L. De Cola, *Adv. Funct. Mater.*, 2009, **19**, 2607-2614.
9. (a) C. H. Chien, S. F. Liao, C. H. Wu, C. F. Shu, S. Y. Chang, Y. Chi, P. T. Chou and C. H. Lai, *Adv. Funct. Mater.*, 2008, **18**, 1430-1439; (b) G. Angulo, A. Kapturkiewicz, S. Y. Chang and Y. Chi, *Inorg. Chem. Commun.*, 2009, **12**, 378-381; (c) B. Carlson, B. E. Eichinger, W. Kaminsky, J. P. Bullock and G. D. Phelan, *Inorg. Chim. Acta*, 2009, **362**, 1611-1618; (d) T. C. Lee, J. Y. Hung, Y. Chi, Y. M. Cheng, G. H. Lee, P. T. Chou, C. C. Chen, C. H. Chang and C. C. Wu, *Adv. Funct. Mater.*, 2009, **19**, 2639-2647.
10. (a) C. A. Strassert, M. Mauro and L. De Cola, in *Adv. Inorg. Chem.*, eds. E. Rudi van and S. Grażyna, Academic Press, 2011, vol. 63, pp. 47-103; (b) M. Mydlak, M. Mauro, F. Polo, M. Felicetti, J. Leonhardt, G. Diener, L. De Cola and C. A. Strassert, *Chem. Mater.*, 2011, **23**, 3659-3667; (c) S. D. Cummings and R. Eisenberg, *J. Am. Chem. Soc.*, 1996, **118**, 1949-1960; (d) S. Develay, O. Blackburn, A. L. Thompson and J. A. Williams, *Inorg. Chem.*, 2008, **47**, 11129-11142; (e) B. W. Ma, P. I. Djurovich, S. Garon, B. Alleyne and M. E. Thompson, *Adv. Funct. Mater.*, 2006, **16**, 2438-2446; (f) J. Schneider, P. Du, X. Wang, W. W. Brennessel and R. Eisenberg, *Inorg. Chem.*, 2009, **48**, 1498-1506; (g) Y. Unger, D. Meyer and T. Strassner, *Dalton Trans.*, 2010, **39**, 4295-4301; (h) Y. Unger, A. Zeller, M. A. Taige and T. Strassner, *Dalton Trans.*, 2009, 4786-4794; (i) Y. Zhang, J. Clavadetscher, M. Bachmann, O. Blacque and K. Venkatesan, *Inorg. Chem.*, 2014, **53**, 756-771; (j) C. Cebrian, M. Mauro, D. Kourkoulos, P. Mercandelli, D. Hertel, K. Meerholz, C. A. Strassert and L. De Cola, *Adv. Mater.*, 2013, **25**, 437-442.
11. (a) O. Elbjeirami, M. D. Rashdan, V. Nesterov and M. A. Rawashdeh-Omary, *Dalton Trans.*, 2010, **39**, 9465-9468; (b) C. Bronner and O. S. Wenger, *Dalton Trans.*, 2011, **40**, 12409-12420; (c) A. Herbst, C. Bronner, P. Dechambenoit and O. S. Wenger, *Organometallics*, 2013, **32**, 1807-1814.
12. (a) A. J. Miller, J. L. Dempsey and J. C. Peters, *Inorg. Chem.*, 2007, **46**, 7244-7246; (b) L. Bergmann, J. Friedrichs, M. Mydlak, T. Baumann, M. Nieger and S. Brase, *Chem. Commun.*, 2013, **49**, 6501-6503; (c) D. Volz, T. Baumann, H. Flugge, M. Mydlak, T. Grab, M. Bachle, C. Barner-Kowollik and S. Brase, *J. Mater. Chem.*, 2012, **22**, 20786-20790.
13. (a) H. J. Son, W. S. Han, J. Y. Chun, B. K. Kang, S. N. Kwon, J. Ko, S. J. Han, C. Lee, S. J. Kim and S. O. Kang, *Inorg. Chem.*, 2008, **47**, 5666-5676; (b) K. A. Truesdell and G. A. Crosby, *J. Am. Chem. Soc.*, 1985, **107**, 1787-1788.
14. K. W. Wang, J. L. Chen, Y. M. Cheng, M. W. Chung, C. C. Hsieh, G. H. Lee, P. T. Chou, K. Chen and Y. Chi, *Inorg. Chem.*, 2010, **49**, 1372-1383.
15. (a) H. D. Velazquez and F. Verpoort, *Chem. Soc. Rev.*, 2012, **41**, 7032-7060; (b) A. R. Naziruddin, C. S. Zhuang, W. J. Lin

and W. S. Hwang, *Dalton Trans.*, 2014, **43**, 5335-5342; (c) A. R. Naziruddin, Z. J. Huang, W. C. Lai, W. J. Lin and W. S. Hwang, *Dalton Trans.*, 2013, **42**, 13161-13171; (d) P. G. Edwards and F. E. Hahn, *Dalton Trans.*, 2011, **40**, 10278-10288; (e) D. Canseco-Gonzalez, A. Petronilho, H. Mueller-Bunz, K. Ohmatsu, T. Ooi and M. Albrecht, *J. Am. Chem. Soc.*, 2013, **135**, 13193-13203.

16. (a) W. A. Herrmann, *Angew. Chem. Int. Ed.*, 2002, **41**, 1290-1309; (b) S. Diez-Gonzalez, N. Marion and S. P. Nolan, *Chem. Rev.*, 2009, **109**, 3612-3676; (c) F. E. Hahn and M. C. Jahnke, *Angew. Chem. Int. Ed.*, 2008, **47**, 3122-3172; (d) J. C. Lin, R. T. Huang, C. S. Lee, A. Bhattacharyya, W. S. Hwang and I. J. B. Lin, *Chem. Rev.*, 2009, **109**, 3561-3598.
17. (a) K. Li, X. Guan, C. W. Ma, W. Lu, Y. Chen and C. M. Che, *Chem Commun.*, 2011, **47**, 9075-9077; (b) V. Leigh, W. Ghattas, R. Lalrempuia, H. Müller-Bunz, M. T. Pryce and M. Albrecht, *Inorg. Chem.*, 2013, **52**, 5395-5402; (c) A. R. Naziruddin, C.-L. Kuo, W.-J. Lin, W.-H. Lo, C.-S. Lee, B.-J. Sun, A. H. H. Chang and W.-S. Hwang, *Organometallics*, 2014, **33**, 2575-2582; (d) Y.-M. C. Chiung-Fang Chang, Yun Chi, Yuan-Chieh Chiu, Chao-Chen Lin, Gene-Hsiang Lee, Pi-Tai Chou, Chung-Chia Chen, Chih-Hao Chang, and Chung-Chih Wu, *Angew. Chem. Int. Ed.* , 2008, **47**, 4542 -4545; (e) R. Visbal and M. C. Gimeno, *Chem. Soc. Rev.*, 2014, **43**, 3551-3574.
18. Y. Unger, A. Zeller, S. Ahrens and T. Strassner, *Chem Commun.*, 2008, 3263-3265.
19. X. F. Zhang, A. M. Wright, N. J. DeYonker, T. K. Hollis, N. I. Hammer, C. E. Webster and E. J. Valente, *Organometallics*, 2012, **31**, 1664-1672.
20. (a) C. S. Lee, S. Sabiah, J. C. Wang, W. S. Hwang and I. J. B. Lin, *Organometallics*, 2010, **29**, 286-289; (b) C. S. Lee, R. R. Zhuang, S. Sabiah, J. C. Wang, W. S. Hwang and I. J. B. Lin, *Organometallics*, 2011, **30**, 3897-3900.
21. Y. Unger, D. Meyer, O. Molt, C. Schildknecht, I. Münster, G. Wagenblast and T. Strassner, *Angew. Chem. Int. Ed.*, 2010, **49**, 10214-10216.
22. Y. C. Chiu, Y. Chi, J. Y. Hung, Y. M. Cheng, Y. C. Yu, M. W. Chung, G. H. Lee, P. T. Chou, C. C. Chen, C. C. Wu and H. Y. Hsieh, *ACS Appl. Mater. Interfaces*, 2009, **1**, 433-442.
23. B. Zhang, L. Zhang, C. Liu, Y. Zhu, M. Tang, C. Du and M. Song, *Dalton Trans.*, 2014, **43**, 7704-7707.
24. (a) U. J. Scheele, M. John, S. Dechert and F. Meyer, *Eur. J. Inorg. Chem.*, 2008, 373-377; (b) Jens C. Röder, F. Meyer, M. Konrad, S. Sandhöfner, E. Kaifer and H. Pritzkow, *Eur. J. Org. Chem.*, 2001, 4479-4487.
25. O. Lohse, P. Thevenin and E. Waldvogel, *Synlett*, 1999, **1999**, 45-48.
26. E. Orselli, G. S. Kottas, A. E. Konradsson, P. Coppo, R. Frohlich, L. De Cola, A. van Dijken, M. Buchel and H. Borner, *Inorg. Chem.*, 2007, **46**, 11082-11093.
27. N. Ghavale, A. Wadawale, S. Dey and V. K. Jain, *J. Organomet. Chem.*, 2010, **695**, 1237-1245.
28. (a) A. Bossi, A. F. Rausch, M. J. Leitl, R. Czerwieniec, M. T. Whited, P. I. Djurovich, H. Yersin and M. E. Thompson, *Inorg. Chem.*, 2013, **52**, 12403-12415; (b) H. Uesugi, T. Tsukuda, K. Takao and T. Tsubomura, *Dalton Trans.*, 2013, **42**, 7396-7403.
29. C. M. Cardona, W. Li, A. E. Kaifer, D. Stockdale and G. C. Bazan, *Adv. Mater.*, 2011, **23**, 2367-2371.
30. (a) J. P. Perdew, K. Burke and M. Ernzerhof, *Phys. Rev. Lett.*, 1996, **77**, 3865-3868; (b) J. P. Perdew, K. Burke and M. Ernzerhof, *Phys. Rev. Lett.*, 1997, **78**, 1396-1396.
31. M. M. Francl, *J. Chem. Phys*, 1982, **77**, 3654.
32. (a) M. E. Casida, C. Jamorski, K. C. Casida and D. R. Salahub, *J. Chem. Phys.*, 1998, **108**, 4439; (b) R. E. Stratmann, G. E. Scuseria and M. J. Frisch, *J Chem Phys*, 1998, **109**, 8218-8224.
33. M. J. Frisch, G. W. Trucks, H. B. Schlegel, G. E. Scuseria, M. A. Robb, J. R. Cheeseman, G. Scalmani, V. Barone, B. Mennucci, G. A. Petersson, H. Nakatsuji, M. Caricato, X. Li, H. P. Hratchian, A. F. Izmaylov, J. Bloino, G. Zheng, J. L. Sonnenberg, M. Hada, M. Ehara, K. Toyota, R. Fukuda, J. Hasegawa, M. Ishida, T. Nakajima, Y. Honda, O. Kitao, H. Nakai, T. Vreven, J. A. Montgomery, Jr., J. E. Peralta, F. Ogliaro, M. Bearpark, J. J. Heyd, E. Brothers, K. N. Kudin, V. N. Staroverov, R. Kobayashi, J. Normand, K. Raghavachari, A. Rendell, J. C. Burant, S. S. Iyengar, J. Tomasi, M. Cossi, N. Rega, J. M. Millam, M. Klene, J. E. Knox, J. B. Cross, V. Bakken, C. Adamo, J. Jaramillo, R. Gomperts, R. E. Stratmann, O. Yazyev, A. J. Austin, R. Cammi, C. Pomelli, J. W. Ochterski, R. L. Martin, K. Morokuma, V. G. Zakrzewski, G. A. Voth, P. Salvador, J. J. Dannenberg, S. Dapprich, A. D. Daniels, O. Farkas, J. B. Foresman, J. V. Ortiz, J. Cioslowski and D. J. Fox, 09 edn., 2009, vol. Gaussian.
34. Z. Otwinowski and W. Minor, in *Methods in Enzymology*, ed. Charles W. Carter, Jr., Academic Press, 1997, vol. 276, pp. 307-326.
35. Z. Otwinowski, D. Borek, W. Majewski and W. Minor, *Acta Crystallogr A*, 2003, **59**, 228-234.
36. G. M. Sheldrick, *Acta Cryst. A*, 1990, **46**, 467-473.
37. G. M. Sheldrick, *Acta Cryst. A*, 2008, **64**, 112-122.

Author Affiliation:
[⊥]Westfälische Wilhelms-Universität Münster, Physikalisches Institut-Center for Nanotechnology, Heisenbergstr. 11, 48149 Münster, Germany; [|]Westfälische Wilhelms-Universität Münster, Organisch-Chemisches Institut, Corrensstr. 40, 48149 Münster, Germany; *Corresponding author; [∇]Current address: Université de Strasbourg, Institut de Science et d'Ingénierie Supramoléculaires, 8 allée Gaspard Monge, 67000 Strasbourg, France. Email: decola@unistra.fr

[†]**Electronic Supplementary Information (ESI) available:** Description of the synthetic procedure for compound **6**; crystallographic refinement parameters and CIF files of all the crystal structures reported herein ; structures are deposited in CCDC database with indexing numbers-CCDC 981765-981767; ambient temperature *Vs* 77K excitation spectra of all complexes; solid state neat film emission spectra of all complexes; list of selected molecular orbital energies [eV] for all complexes and HOMO–LUMO energy gaps; isodensity surfaces plots of selected orbitals

for all complexes; cyclic voltammetry plots. This material is available free of charge via the Internet at http://pubs.rsc.org.
See DOI: 10.1039/b000000x/

TOC Graphics:

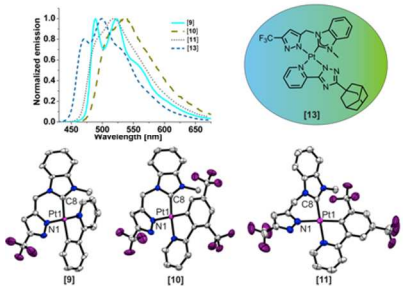

Text for TOC content:

Platinum complexes containing NHC^pyrozolate ligands and functionalized-phenyl-pyridine or triazole-pyridine^{Ad} chromophores are reported. All the compounds are luminescent and their emission can be tuned from blue to yellow.